pISSN 2384-1095
eISSN 2384-1109

iMRI 2018;22:123-130

https://doi.org/10.13104/imri.2018.22.2.123

iMRI
Investigative Magnetic Resonance Imaging

MRI Findings of an Ampulla of Vater Neuroendocrine Tumor with Liver and Lymph Node Metastasis: a Case Report

Jung Hyun Noh[1], **Mi Hyun Park**[1], **Seung Kyu Choi**[2]

[1]Department of Radiology, Dankook University Hospital, Dankook University School of Medicine, Cheonan, Korea
[2]Department of Pathology, Dankook University Hospital, Dankook University School of Medicine, Cheonan, Korea

Case Report

Received: April 10, 2018
Revised: May 29, 2018
Accepted: May 30, 2018

Correspondence to:
Mi Hyun Park, M.D.
Department of Radiology, Dankook University Hospital, Dankook University School of Medicine, 201 Manghyang-ro, Dongnam-gu, Cheonan 31116, Korea.
Tel. +82-41-550-3293
Fax. +82-41-552-9674
E-mail: deepva@hanmail.net

An ampulla of Vater neuroendocrine tumor (AOV-NET) is a rare subset of gastroenteropancreatic neuroendocrine tumors (GEP-NETs). Very few studies have been undertaken regarding MRI findings of an AOV-NET. We report on a case of a 59-year-old woman diagnosed with an AOV-NET with liver and lymph node metastasis, with an emphasis on the MRI findings. This case shows rare and precious typical MRI findings of an AOV-NET. The MRI visualized the AOV-NET very well and is helpful for the differentiation of an AOV-NET from other tumors in the ampullary area as well as with treatment planning.

Keywords: Neuroendocrine tumor; Ampulla of Vater; Magnetic resonance imaging (MRI)

INTRODUCTION

Gastroenteropancreatic neuroendocrine tumors (GEP-NETs) are a heterogeneous group of tumors, which arise in the cells of the neuroendocrine system (1). Ampulla of Vater neuroendocrine tumors (AOV-NETs) are an extremely rare subset of GEP-NETs and accounts for 0.3% to 1% of all GEP-NETs (2). Further, AOV-NETs account for less than 2% of ampullary tumors (2-4). About 140 cases of AOV-NETs have been reported (5). However, there are few reports on the MRI findings of AOV-NETs, because AOV-NETs are not only rare, are also usually not evaluated with MRI. Therefore, we report the MRI findings of a rare case of an AOV-NET with liver and lymph node metastasis.

CASE REPORT

A 59-year-old woman with Crohn's disease underwent a follow-up esophagogastroduodenoscopy (EGD) and colonoscopy, which revealed the disease was in remission. However, a focal hyperemic nodular lesion was detected at the duodenal ampulla. Bulging of the duodenal ampulla was noted while preserving the overlying mucosa. Laboratory examination, including total bilirubin and tumor markers, were unremarkable.

An endoscopic ultrasound (EUS) and abdominal CT scan were performed. The EUS showed a 1.5 cm low echoic mass at the ampulla of Vater (AOV). The enhanced pancreatic phase abdominal CT images show a 1.5 cm mass with avid, homogeneous enhancement at the AOV (Fig. 1a), a 9.7 cm lobulated enhancing mass with multifocal low attenuating cystic or necrotic change in the right hepatic lobe, and several small, low attenuating lesions in both hepatic lobes (Fig. 1b). A 2.3 cm enlarged lymph node with prominent enhancement and central necrotic change was noted in the left para-aortic area (Fig. 1c). Considering the EUS and CT findings, an AOV NET was the most likely suggested. In addition, we suggested that the large hepatic mass was a hypervascular liver metastasis of the AOV-NET.

The liver MRI (Ingenia 3.0T, Philips Healthcare, Best, the Netherlands) was performed in order to further evaluate the hepatic metastasis. A dynamic enhancement study, using Gd-EOB-DTPA (Primovist), was performed. The AOV mass manifested as a 1.5 cm round lesion with slightly high signal intensity when compared with a pancreatic parenchyma on a T2-weighted image (Fig. 2a) and low signal intensity on a T1-weighted image (Fig. 2b). The AOV mass showed avid, homogeneous enhancement on the arterial phase (Fig. 2c) and isosignal intensity when compared with a pancreatic parenchyma on the delayed phase (Fig. 2d). The AOV mass exhibited a high signal intensity on a high b value diffusion-weighted image (Fig. 2e) without a definitive low apparent diffusion coefficient (ADC) value (Fig. 2f). The common bile duct and the main pancreatic duct were mildly dilated.

The single hepatic mass showed a ring-like, radial appearance and strong enhancement with multifocal low signal intensity cystic portions on the arterial phase (Fig. 3a) of the enhanced liver MRI. The hepatic mass showed heterogeneous isosignal intensity, than liver parenchyma on

a

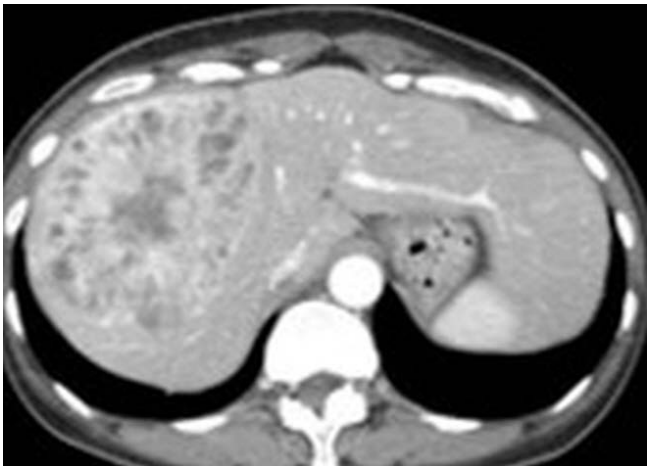

b

c

Fig. 1. A 59-year-old woman with an ampulla of Vater (AOV) neuroendocrine tumor. The enhanced pancreatic phase abdominal CT images show (a) a 1.5 cm mass (arrow) with avid, homogeneous enhancement at the AOV, (b) a 9.7 cm lobulated enhancing mass with multifocal low attenuating cystic or necrotic change in the right hepatic lobe and (c) a 2.3 cm enlarged lymph node (arrow) with central necrotic change was noted in the left para-aortic area.

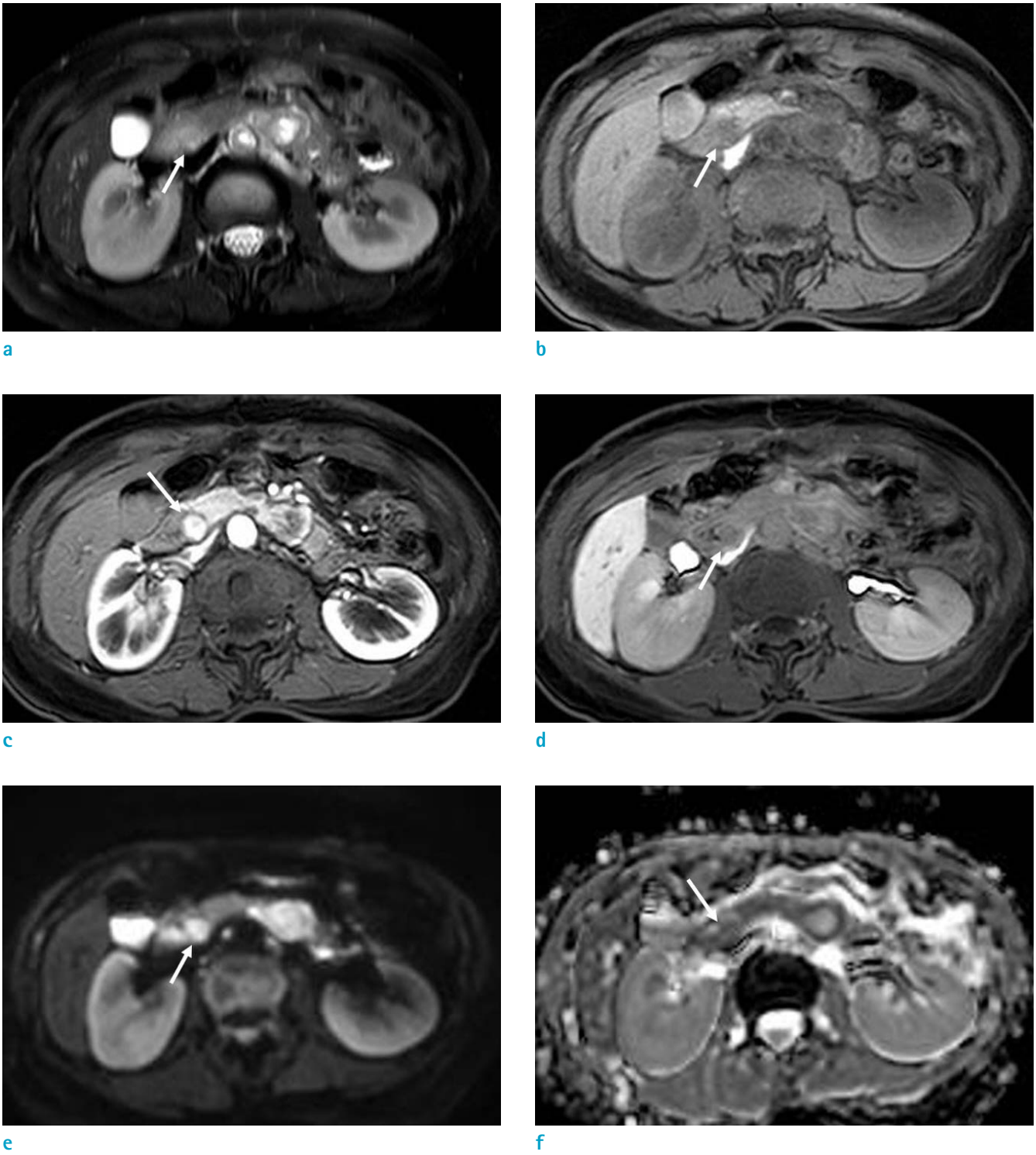

Fig. 2. An ampulla of Vater (AOV) neuroendocrine tumor in a 59-year-old woman. A 1.5 cm sized round mass in the AOV (arrow) showed slightly high signal intensity when compared with a pancreatic parenchyma on a T2-weighted image (a) and low signal intensity on a T1-weighted image (b). On the enhanced MRI, using GD-EOB-DTPA (Primovist), the AOV mass (arrow) showed avid, homogeneous enhancement on the arterial phase (c) with isosignal intensity when compared with a pancreatic parenchyma on the delayed phase (d). The AOV mass (arrow) exhibited high signal intensity on a high b value diffusion weighted image (e) without a definitive low apparent diffusion coefficient value (f).

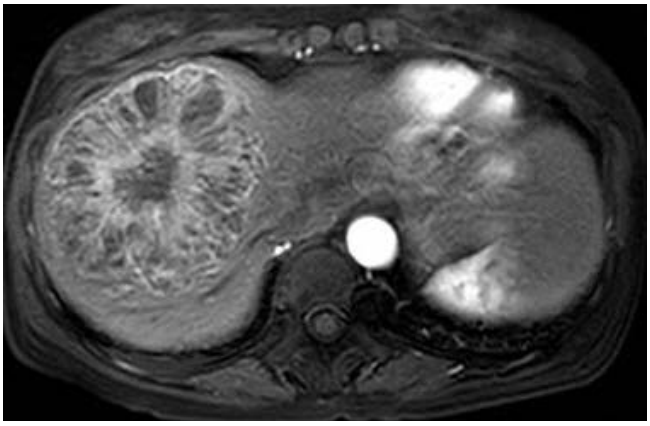
a

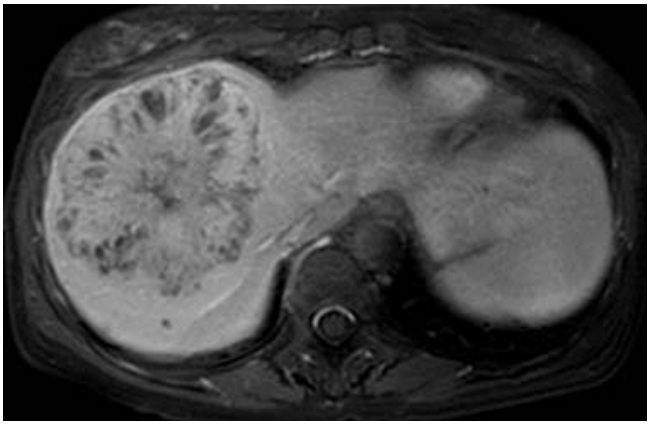
b

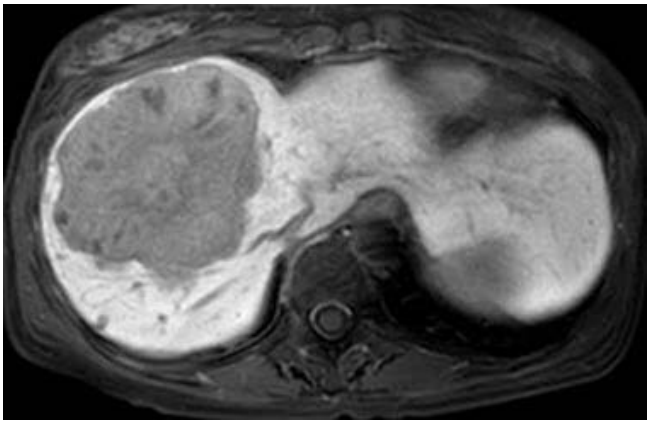
c

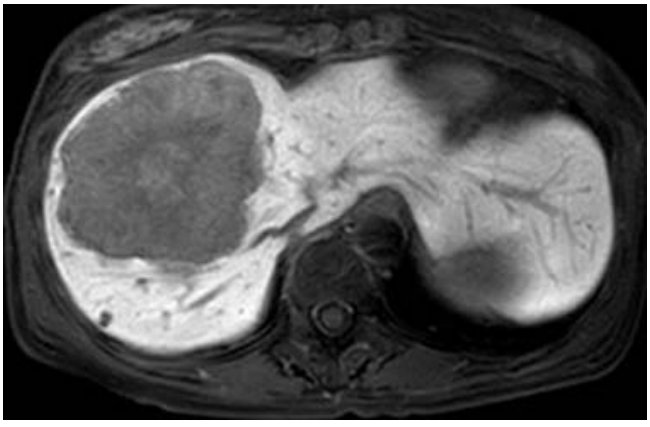
d

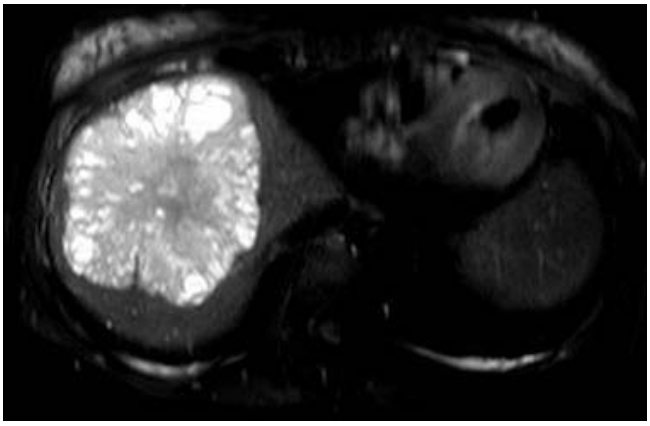
e

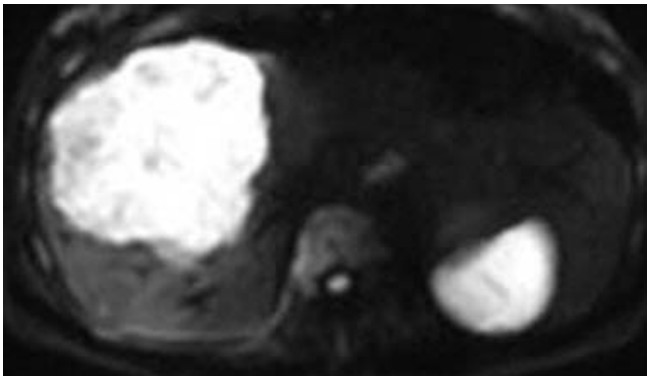
f

Fig. 3. A metastatic hepatic mass in a 59-year-old woman. The single hepatic mass showed a ring like, radial appearance, strong enhancement with multifocal low signal intensity cystic portions on the arterial phase (a) of enhanced MRI. The hepatic mass showed heterogeneous isosignal intensity, than liver parenchyma on the portal-venous phase (b), washout on the delayed phase (c) and low signal intensity on the hepatobiliary phase (d). There were multifocal bright signal intensity cystic lesions in the hepatic mass on a T2-weighted image (e).

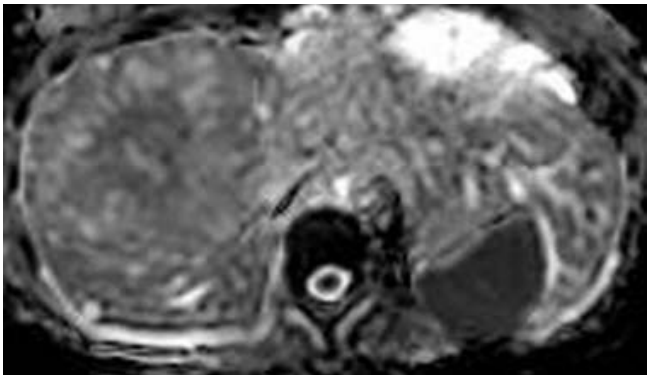

g

Fig. 3. The hepatic mass showed high signal intensity on a diffusion weighted image (f) without a definite low apparent diffusion coefficient value (g).

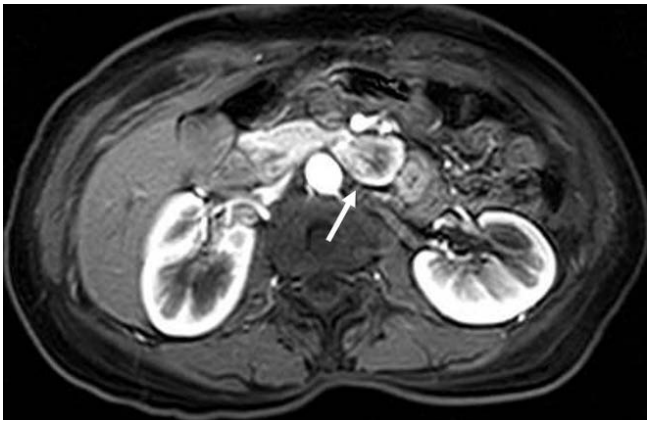

a

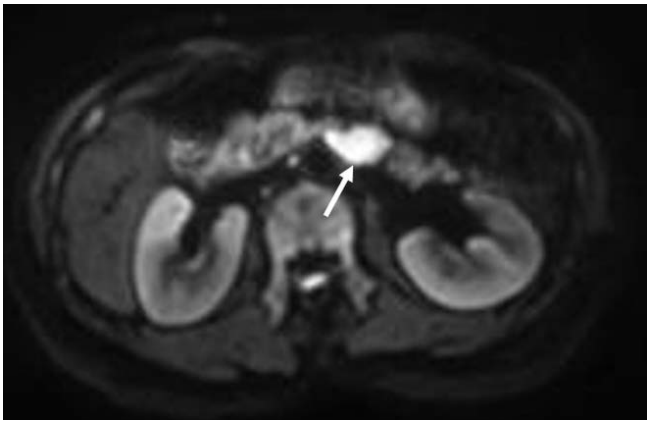

b

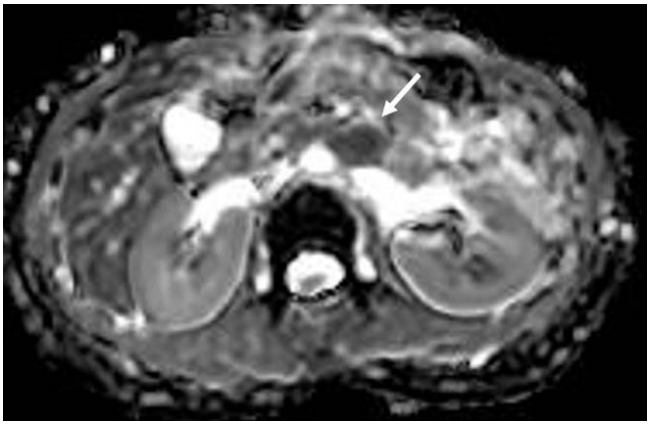

c

Fig. 4. A metastatic paraaortic lymph node in a 59-year-old woman. An enlarged lymph node (arrow) with a central necrotic portion was noted in the left para-aortic area. This lymph node showed prominent enhancement on the arterial phase of an enhanced MRI (a). The enhanced portion of this lymph node (arrow) showed high signal intensity on a diffusion weighted image (b) and a low apparent diffusion coefficient value (c).

the portal-venous phase (Fig. 3b), washout on the delayed phase (Fig. 3c), and low signal intensity on the hepatobiliary phase (Fig. 3d). There were multifocal, bright-signal intensity cystic lesions in the hepatic mass on a T2-weighted image (Fig. 3e). The hepatic mass showed a high signal intensity on a diffusion-weighted image (Fig. 3f), without definite low ADC value (Fig. 3g). The liver MRI revealed that several small, low attenuating lesions, previously noted on the CT scan, were T2 bright signal intensity cysts.

Further, an enlarged lymph node with a central necrotic portion was noted in the left para-aortic area. This lymph node showed prominent enhancement on the arterial phase

of an enhanced MRI (Fig. 4a). Enhanced portions of the lymph node showed high signal intensity on a diffusion-weighted image (Fig. 4b), and low ADC value (Fig. 4c), which indicate a diffusion restriction.

An endoscopic biopsy was performed for the mass and an AOV and ultrasonography-guided percutaneous biopsy was performed for the liver mass. Pathologic examination confirmed the AOV mass as a NET and the liver mass as a metastatic NET.

The patient underwent a right hepatectomy, pylorus-preserving pancreatico-duodenectomy, and lymph node dissection. The gross specimen showed a 1.5 cm well-demarcated whitish solid mass at the AOV (Fig. 5a) and a 9.0 cm well-demarcated red tan mass with a fish-flesh consistency in the right hepatic lobe (Fig. 5b). Upon microscopic examination (Hematoxylin & Eosin staining, × 100), the tumor cells of the AOV mass showed nested (Fig. 5c), trabecular growth patterns as well as moderate amounts of cytoplasm and round nuclei. Immunostaining for synaptophysin was positive in the tumor cells (Fig. 5d). Microscopic examination confirmed the AOV mass as a NET. No invasion to the pancreas head, common bile duct, or duodenum was observed. The liver mass and left para-aortic lymph node were confirmed as a metastatic NET.

DISCUSSION

The incidence of GEP-NETs has increased in recent years, due to improved imaging techniques and the increased use of endoscopy. However, AOV-NETs are very rare (5). AOV NETs are considered to have several biologic features

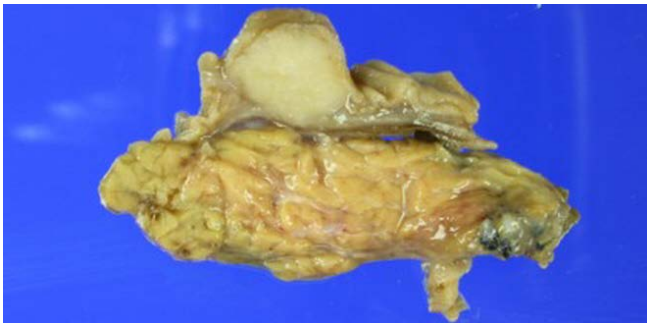

a

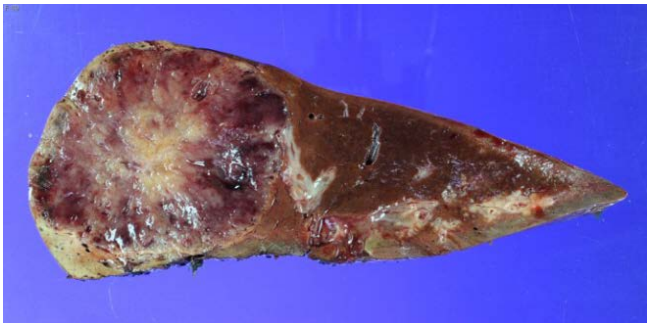

b

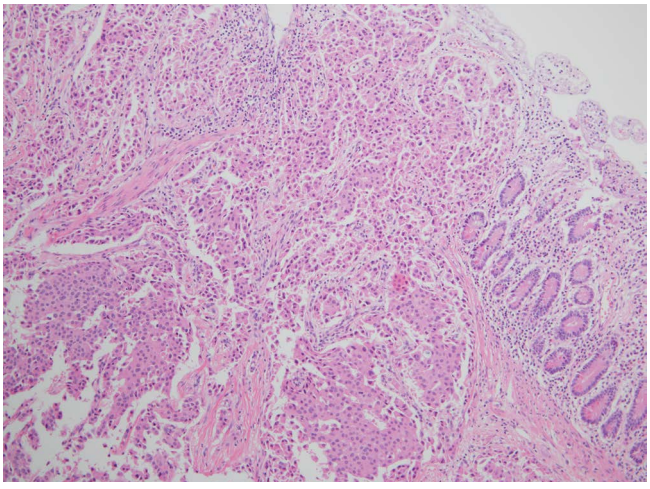

c

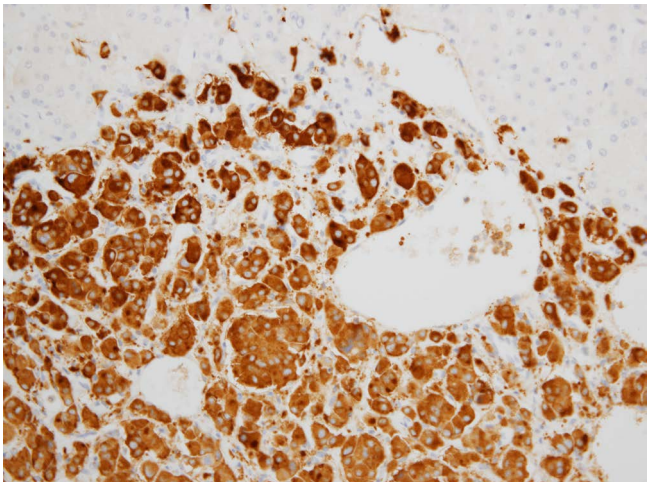

d

Fig. 5. The gross specimen and microscopic examination. The gross specimen showed (a) a 1.5 cm well-demarcated whitish solid mass at the ampulla of Vater (AOV) and (b) a 9.0 cm well-demarcated red tan mass with a fish-flesh consistency in the right hepatic lobe. Upon microscopic examination (Hematoxylin & Eosin staining, × 100), the tumor cells of the AOV mass showed (c) a nested, trabecular growth pattern and had moderate amounts of cytoplasm and round nuclei. Immunostaining for synaptophysin was positive in the tumor cells (d).

when compared with other GEP-NETs. AOV-NETs are considered more likely to present as small lesions, with a high tendency of metastasis (6). However, the natural history and prognostic factors of an AOV-NET have yet to be established. Therefore, there are no standard treatments for AOV NETs. Pancreatico-duodenectomy is considered to be the treatment of choice. However, a few studies suggest endoscopic local resection and surgical ampullectomy for well-differentiated, small AOV-NETs (less than 2 cm) and patients with a high surgical risk (3-5). Endoscopic retrograde cholangiopancreatography (ERCP) and EUS are commonly used for the evaluation of ampullary lesions, including AOV-NETs. EUS facilitates the evaluation of the depth of invasion from an AOV-NET (2). Abdominal CT and MRI are generally used in order to evaluate metastasis, but not to evaluate the ampullary lesion itself, because small ampullary lesions are usually poorly visualized on a CT and MRI (2).

The MRI finding of a GEP-NET is mostly a hypervascular tumor, which is apparent as a high enhancement on the arterial phase. These tumors show varying degrees of heterogeneity, such as cystic or necrotic change, depending on the tumor size and behavior. Large and fast-growing NETs are more likely to show heterogeneity. NETs show low signal intensity on a T1-weighted image and high signal intensity on a T2-weighted image (1, 7). Further, the reported CT findings of AOV-NETs are hypervascular masses at the AOV with or without dilatation of the common bile and main pancreatic duct (6, 8). The AOV-NET was well visualized on the MRI as a small, homogeneous hypervascular masses in the AOV, which is a typical imaging feature of a NET in the present case.

In a NET, liver metastasis is most common after lymph node metastasis and is important for staging, prognosis, and treatment planning (1, 7, 9). Therefore, accurate evaluation is important for liver metastasis in an AOV-NET. Similar to the imaging findings of a primary NET, liver metastasis manifests as a hypervascular mass on the arterial phase with washout on the delayed phase of a CT or MRI (7). Liver metastasis manifests as a low signal intensity lesion on the hepatobiliary phase using a hepatocyte-specific agent. In addition, a larger lesion typically manifests as a ring-like or radial heterogeneous enhancement with cystic or necrotic areas (1, 7, 10). In the present case, hepatic metastasis manifested as a large hypervascular mass with multifocal T2 bright signal intensity cystic portions. The MRI revealed the hepatic metastasis as a single lesion confined to the right hepatic lobe and the surgeon could consider a curative right hepatectomy.

The lymph node is the most common site of metastasis in a NET (1, 9). Lymph node metastasis is related to prognosis in a pancreatic NET. However, some studies have reported that lymph node metastasis is not correlated with prognosis in an AOV-NET, warranting further investigations. Lymph node metastasis of a NET shows prominent enhancement on a CT or MRI and may show necrotic change (7). In the present case, a prominent enhancing hypervascular metastatic lymph node with a necrotic portion was noted on the arterial phase of MRI. Also, this lymph node showed diffusion restriction.

In conclusion, as a hypervascular mass in an AOV with hypervascular liver and lymph node metastasis on the MRI, the present case shows rare and precious typical MRI findings of an AOV-NET. The MRI visualized the AOV-NET very well and can be helpful with the differentiation of an AOV-NET from other tumors in the ampullary area as well as for treatment planning.

REFERENCES

1. Sahani DV, Bonaffini PA, Fernandez-Del Castillo C, Blake MA. Gastroenteropancreatic neuroendocrine tumors: role of imaging in diagnosis and management. Radiology 2013;266:38-61
2. Jayant M, Punia R, Kaushik R, et al. Neuroendocrine tumors of the ampulla of vater: presentation, pathology and prognosis. JOP 2012;13:263-267
3. Carter JT, Grenert JP, Rubenstein L, Stewart L, Way LW. Neuroendocrine tumors of the ampulla of Vater: biological behavior and surgical management. Arch Surg 2009;144:527-531
4. Dumitrascu T, Dima S, Herlea V, Tomulescu V, Ionescu M, Popescu I. Neuroendocrine tumours of the ampulla of Vater: clinico-pathological features, surgical approach and assessment of prognosis. Langenbecks Arch Surg 2012;397:933-943
5. Yang K, Yun SP, Kim S, Shin N, Park DY, Seo HI. Clinicopathological features and surgical outcomes of neuroendocrine tumors of ampulla of Vater. BMC Gastroenterol 2017;17:70
6. Raman SP, Fishman EK. Abnormalities of the distal common bile duct and ampulla: diagnostic approach and differential diagnosis using multiplanar reformations and 3D imaging. AJR Am J Roentgenol 2014;203:17-28
7. Lewis RB, Lattin GE Jr, Paal E. Pancreatic endocrine tumors: radiologic-clinicopathologic correlation. Radiographics

2010;30:1445-1464
8. Tsukagoshi M, Hosouchi Y, Araki K, et al. Neuroendocrine tumor of the ampulla of Vater with distant cystic lymph node metastasis: a case report. Surg Case Rep 2016;2:73
9. Saeed A, Buell JF, Kandil E. Surgical treatment of liver metastases in patients with neuroendocrine tumors. Ann Transl Med 2013;1:6
10. Dromain C, de Baere T, Baudin E, et al. MR imaging of hepatic metastases caused by neuroendocrine tumors: comparing four techniques. AJR Am J Roentgenol 2003;180:121-128